Neuron, Volume *104*

Supplemental Information

CRISPR-Cas9 Screens Identify the RNA Helicase DDX3X as a Repressor of *C9ORF72* (GGGGCC)n Repeat-Associated Non-AUG Translation

Weiwei Cheng, Shaopeng Wang, Zhe Zhang, David W. Morgens, Lindsey R. Hayes, Soojin Lee, Bede Portz, Yongzhi Xie, Baotram V. Nguyen, Michael S. Haney, Shirui Yan, Daoyuan Dong, Alyssa N. Coyne, Junhua Yang, Fengfan Xian, Don W. Cleveland, Zhaozhu Qiu, Jeffrey D. Rothstein, James Shorter, Fen-Biao Gao, Michael C. Bassik, and Shuying Sun

Inventory of Supplemental Information

I. Supplemental Figures

II. Supplemental Tables

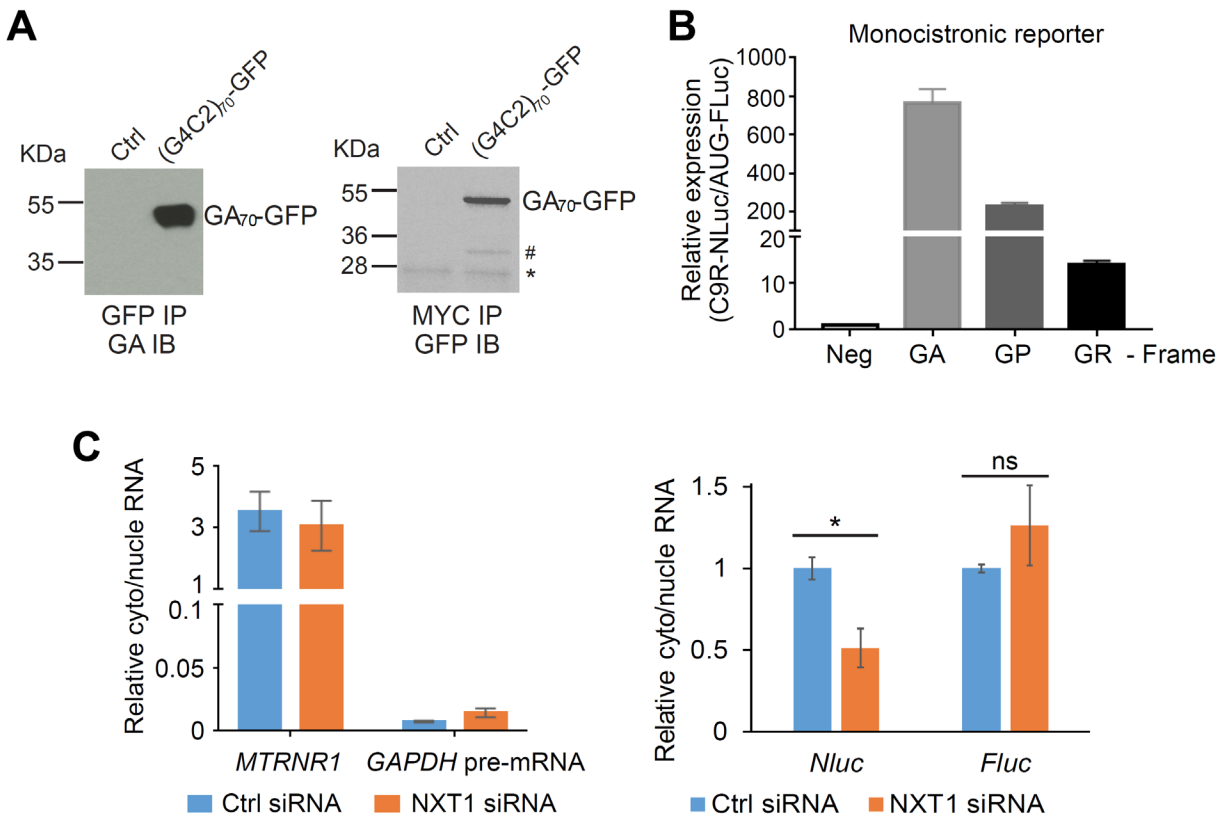

Figure S1: C9ORF72 repeat translation reporter cells and the NXF1-NXT1 pathway mediates repeat RNA export. Related to Figure 1,2.

(A) Immunoprecipitation (IP) using GFP or MYC antibody from the RPE-1 C9R-EGFP GA-frame reporter cells, followed by immunoblotting (IB) with GA or GFP antibody. *non-specific band. #a shorter product that might be GFP-MYC only.

(B) The relative levels of C9R-NLuc in the three reading frames. HeLa Flp-In reporter cells were induced to express the translation reporters by doxycycline for 24 hours. Relative RAN translation products from GA, GP and GR frames were compared to no-repeat control. NLuc signals were normalized to FLuc in each sample. Data are mean ± s.e.m. from three biological replicates.

(C) Relative cytoplasmic/nuclear RNAs were measured by qRT-PCR. HeLa Flp-In cells of monocistronic reporter cells were induced to express translation reporters by doxycycline after two days of siRNA transfection, and fractionated to separate nucleus and cytoplasm after another 24 hours. The levels of each RNA were measured by qRT-PCR and normalized to GAPDH mRNA in each fraction. The ratio of cytosolic/nuclear RNA showed the sub-cellular distribution of each RNA. The relative cytosolic/nuclear ratio of each gene in the NXT1 knockdown condition was then compared with the non-targeting siRNA control. Data are mean ± s.e.m. from three biological replicates. *P<0.05, two-tailed t test.

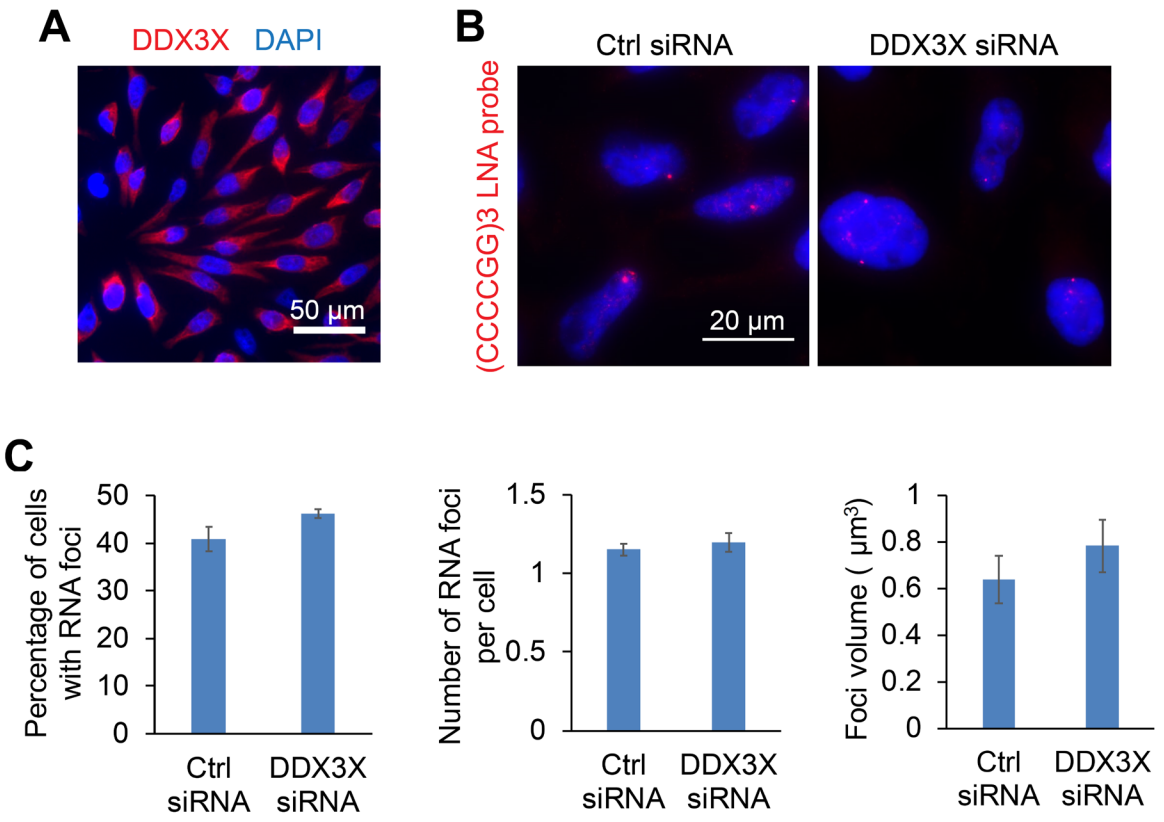

Figure S2: DDX3X does not affect repeat-containing RNA foci in the nucleus. Related to Figure 3.

(A) Immunofluorescence of endogenous DDX3X showed its predominant localization in cytoplasm. The scale bar represents 50 μm.

(B) RNA fluorescence in situ hybridization for GGGGCC repeat RNA foci in HeLa Flp-In reporter cells transfected with either control or DDX3X siRNA. The scale bar represents 20 μm.

(C) Quantification of nuclear RNA foci number and size in (B). More than 200 cells were counted in each condition. Data are mean ± s.e.m. from three biological replicates.

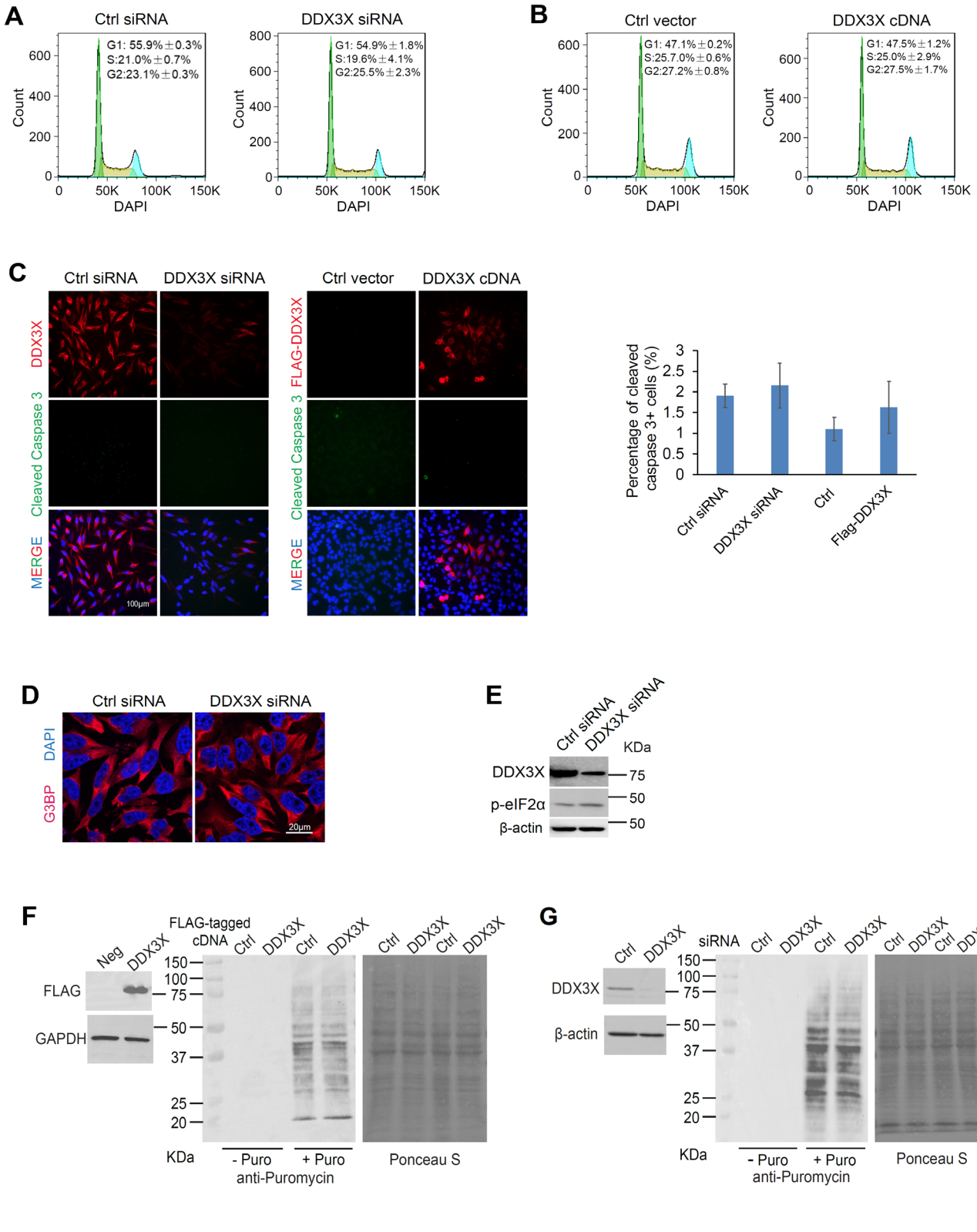
A
Ctrl siRNA
DDX3X siRNA
G1: 55.9%±0.3%
S:21.0%±0.7%
G2:23.1%±0.3%
G1: 54.9%±1.8%
S:19.6%±4.1%
G2:25.5%±2.3%
Count
DAPI
B
Ctrl vector
DDX3X cDNA
G1: 47.1%±0.2%
S:25.7.0%±0.6%
G2:27.2%±0.8%
G1: 47.5%±1.2%
S:25.0%±2.9%
G2:27.5%±1.7%
C
Ctrl siRNA
DDX3X siRNA
Ctrl vector
DDX3X cDNA
DDX3X
FLAG-DDX3X
Cleaved Caspase 3
MERGE
100μm
Percentage of cleaved caspase 3+ cells (%)
Ctrl siRNA
DDX3X siRNA
Ctrl
Flag-DDX3X
D
Ctrl siRNA
DDX3X siRNA
DAPI
G3BP
20μm
E
Ctrl siRNA
DDX3X siRNA
KDa
DDX3X
p-eIF2α
β-actin
75
50
50
F
Neg
DDX3X
FLAG-tagged cDNA
Ctrl
DDX3X
Ctrl
DDX3X
Ctrl
DDX3X
Ctrl
DDX3X
FLAG
GAPDH
150
100
75
50
37
25
20
KDa
- Puro
+ Puro
anti-Puromycin
Ponceau S
G
Ctrl
DDX3X
siRNA
Ctrl
DDX3X
Ctrl
DDX3X
Ctrl
DDX3X
Ctrl
DDX3X
DDX3X
β-actin
150
100
75
50
37
25
20
KDa
- Puro
+ Puro
anti-Puromycin
Ponceau S

Figure S3: Changes of DDX3X levels did not affect cell proliferation, apoptosis and global protein synthesis in the HeLa reporter cells. Related to Figure 3.

(A) Cells with either control siRNA or DDX3X siRNA transfection were fixed and stained with DAPI, and analyzed by flow cytometry. The area parameter histogram of DAPI was used to determine the percentage of cells in G1, S and G2 phases. Data are mean ± s.e.m. from three biological replicates.

(B) Cell cycle analysis of cells with control or DDX3X cDNA transfection, as in (A).

(C) Cleaved Caspase-3 immunofluorescence of reporter cells with DDX3X knockdown or overexpression. The scale bar represents 100 μm. (Right) The percentage of cleaved Caspase-3 positive cells showed no difference. Error bars represent s.e.m. in three biological replicates.

(D) Immunofluorescence of G3BP showed no stress granule formation upon DDX3X knockdown. The scale bar represents 20 μm.

(E) Immunoblotting of phospho-eIF2α showed DDX3X knockdown did not activate integrated stress response. β-actin was blotted as internal control.

(F, G) Changes of DDX3X levels did not affect global protein synthesis. Puromycin incorporation assay to measure the actively translating nascent polypeptides, when DDX3X was overexpressed (F) or knocked down (G). Ponceau S staining showed the equal amount of total protein.

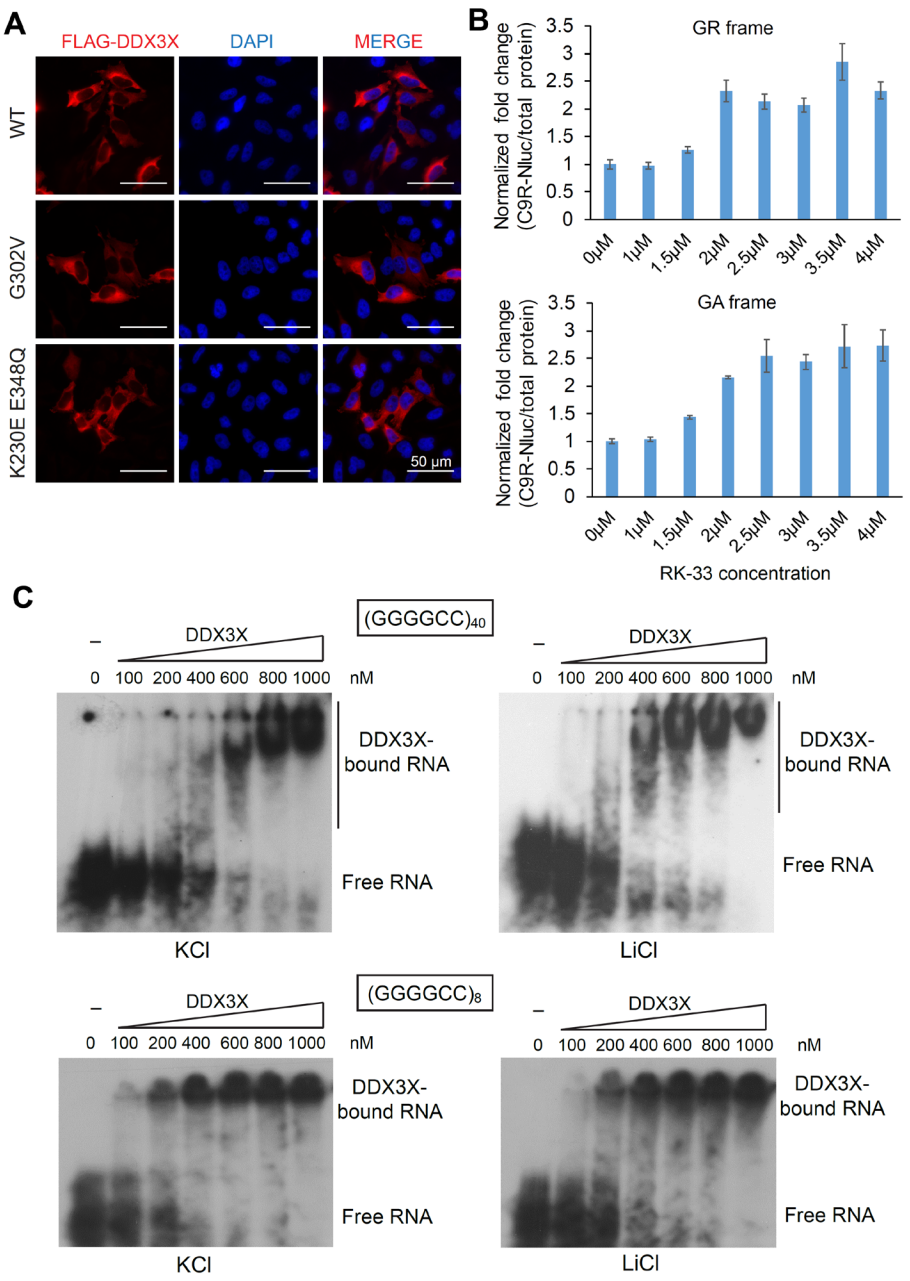

Figure S4: DDX3X binds (GGGGCC)n RNA and modulates RAN translation through helicase activity. Related to Figure 3,4.

(A) Wild type and mutant DDX3X have similar cytosolic localization. FLAG immunofluorescence of HeLa cells transfected with FLAG-tagged DDX3X wild type, G302V, or K230E+E348Q mutant constructs. Scale bars represent 50 μm.

(B) The helicase activity is essential for RAN translation repression. GR and GA reporter cells were treated with increasing dosage of DDX3X ATPase inhibitor RK-33 for 24 h. NLuc signals were normalized to total protein in each sample and the relative expression was compared to DMSO treatment control. Data are mean ± s.e.m. from three biological replicates.

(C) Gel mobility shift assay showed Li^+ does not influence the binding of DDX3X on GGGGCC repeat RNA. The *in vitro* transcribed radiolabeled (GGGGCC)n RNA was incubated with increasing doses of purified DDX3X proteins, in the presence of either KCl or LiCl.

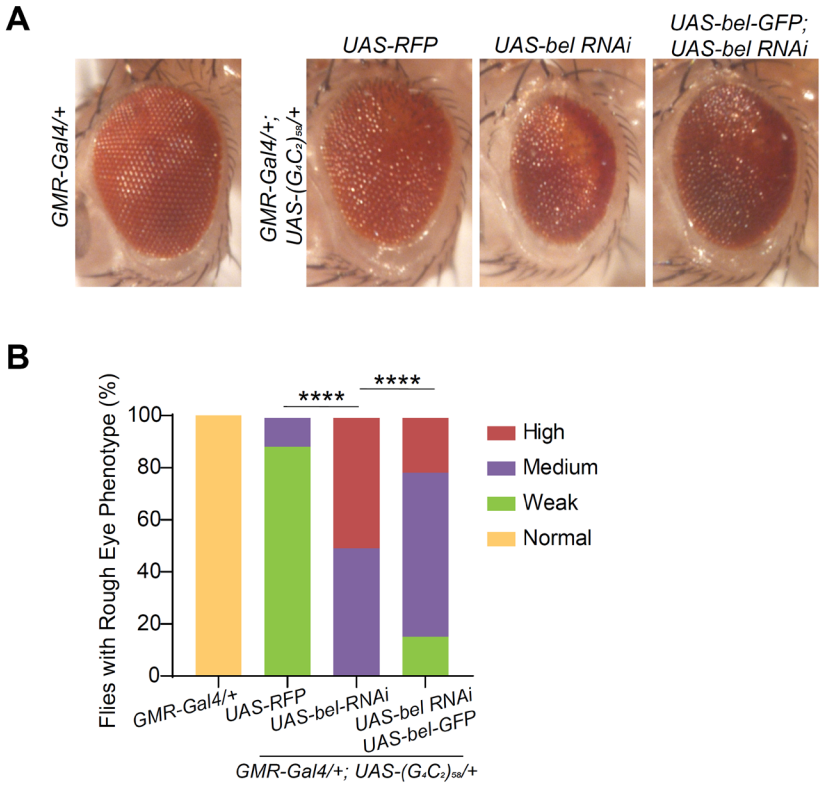

Figure S5: Ectopic Bel expression rescues the enhanced rough eye phenotype caused by partial loss of *bel* function in flies expressing expanded GGGGCC repeats. Related to Figure 5.

(A) Representative images of compound eyes of adult flies with different genotypes. Partial loss of *bel* function through RNAi knockdown (*bel*^{JF02884}) enhances $(G_4C_2)_{58}$ toxicity. Ectopic expression of Bel-GFP partially rescues the rough eye phenotype caused by *bel* knockdown in flies expressing $(G_4C_2)_{58}$. *UAS-RFP* was used as the control for *UAS-bel-GFP*. The genotypes of all flies examined here are described in detail in the Methods section.

(B) Quantification of the rough eye phenotype in flies with different genotypes. ****$P < 0.0001$, by chi-square analysis. The number of flies analyzed for each genotype ranges from 100 to160.

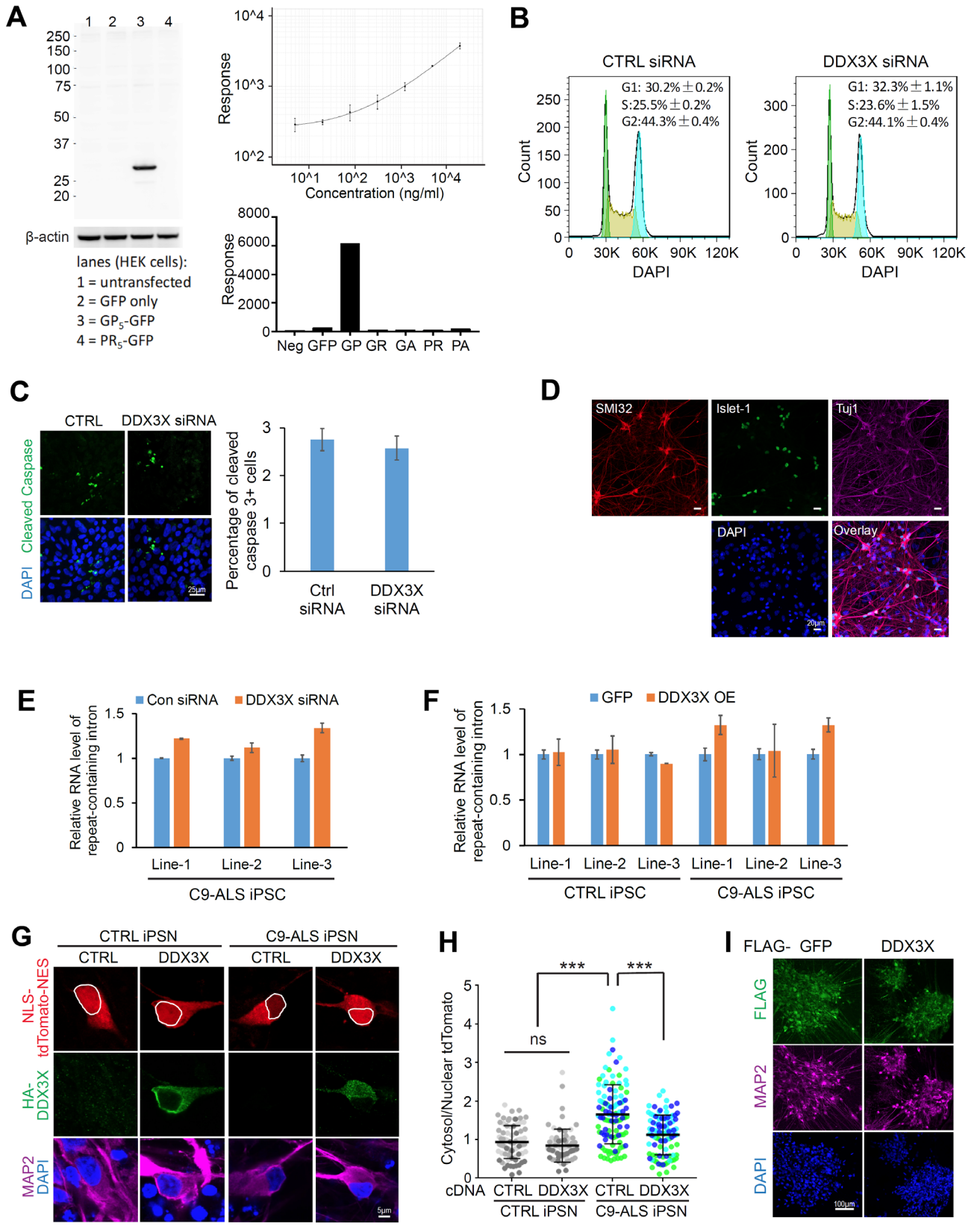
A
1 2 3 4
250
150
100
75
50
37
25
20
β-actin
lanes (HEK cells):
1 = untransfected
2 = GFP only
3 = GP5-GFP
4 = PR5-GFP
Response
Concentration (ng/ml)
Neg GFP GP GR GA PR PA
B
CTRL siRNA
DDX3X siRNA
G1: 30.2%±0.2%
S:25.5%±0.2%
G2:44.3%±0.4%
G1: 32.3%±1.1%
S:23.6%±1.5%
G2:44.1%±0.4%
Count
DAPI
C
CTRL
DDX3X siRNA
Cleaved Caspase
DAPI
Percentage of cleaved caspase 3+ cells
Ctrl siRNA
DDX3X siRNA
D
SMI32
Islet-1
Tuj1
DAPI
Overlay
E
Con siRNA
DDX3X siRNA
Relative RNA level of repeat-containing intron
Line-1
Line-2
Line-3
C9-ALS iPSC
F
GFP
DDX3X OE
CTRL iPSC
C9-ALS iPSC
G
CTRL iPSN
C9-ALS iPSN
CTRL
DDX3X
NLS-tdTomato-NES
HA-DDX3X
MAP2
DAPI
H
Cytosol/Nuclear tdTomato
ns
***
cDNA
I
FLAG- GFP
DDX3X
FLAG
MAP2
DAPI

Figure S6: DDX3X modulates DPR protein levels and DPR-mediated toxicity in patient cells. Related to Figure 6.

(A) *C9ORF72* GP ELISA assay. (Left) Immunoblotting of rabbit anti-GP antibody (5278) on HEK 293 cells transfected with indicated constructs showed the antibody specificity. (Top right) MSD ELISA using serial dilution of synthesized GP_8 peptide showed the linear response of the assay. (Bottom right) MSD ELISA using lysates of HEK 293 cells expressing different DPR_5 showed the specific response for GP.

(B) Cell cycle analysis calculated G1, S and G2 phase from the DAPI-area histogram of iPSCs with either control or DDX3X siRNA transfection, based on three individual lines. Data are mean ± s.e.m. from three biological replicates.

(C) (Left) Cleaved Caspase-3 immunofluorescence of iPSCs transfected with control or DDX3X siRNA. The scale bar represents 25 μm. (Right) The percentage of cleaved Caspase-3 positive cells showed no difference in the DDX3X knockdown cells. Error bars represent s.e.m. in three individual lines.

(D) Immunofluorescence characterization of iPSC-neurons. iPSCs differentiated into motor neurons expressing cell type markers SMI32, Islet-1 and Tuj1. The neurons were plated on astrocyte feeder layer for immunofluorescence. Scale bars represent 20 μm.

(E) *C9ORF72* intron-containing repeat RNA was measured by qRT-PCR in control or DDX3X siRNA transfected iPSCs and normalized to β-actin. Error bars represent s.e.m. in three biological replicates.

(F) *C9ORF72* intron-containing repeat RNA was measured by qRT-PCR in control or DDX3X overexpression iPSNs and normalized to β-actin. Error bars represent s.e.m. in three biological replicates.

(G) Immunofluorescence of exogenously expressed HA-tagged DDX3X, NLS-tdTomato-NES transport reporter, and MAP2 as neuronal marker in iPSC-derived neurons. The scale bar represents 5 μm.

(H) Quantification of neuronal C/N tdTomato ratios in (G) showed decreased nuclear reporter levels in *C9ORF72*-ALS iPSN compared to control, and overexpression of DDX3X increased nuclear tdTomato. Data points of different colors represent individual cells from different lines. 25-40 neurons were quantified at each condition from each line. ***$P<0.001$, one-way ANOVA with Dunn's post hoc test. Data are mean ± s.d. from three *C9ORF72*-ALS iPSN lines and three CTRL iPSN lines.

(I) Immunofluorescence of FLAG tag and MAP2 of iPSNs infected with lentivirus. The scale bar represents 100 μm.

Table S2: Summary of siRNA validation in dual-luciferase reporters-GP frame. Related to Figure 1.

Gene name	C9R-Nluc fold change	AUG-Fluc fold change	Nluc/Fluc fold change	Nluc/Fluc p value
DDX3X	2.238943801	0.656675606	3.409512675	2.86171E-05
DPH5	1.75047811	0.868772616	2.004521849	0.00099638
DDX54	1.221981771	0.905365757	1.349710612	0.013648801
METTL14	1.161316575	0.852288285	1.362586575	0.004931377
DPH6	1.597055441	0.978398663	1.632315641	0.010976193
DHX29	1.133071424	0.755091262	1.500575468	0.000461986
DNAJC24	0.876815077	0.648467161	1.352134896	0.000301592
NXF1	0.615989376	1.552269874	0.2704794	0.002351137
NXT1	0.518024063	1.086237096	0.476897783	0.000443455
PSMA6	0.271237229	0.798136271	0.337257971	0.01699435
THOC3	0.521463674	0.810678545	0.643243462	0.03653937
THOC7	0.615561562	1.012703649	0.607839779	0.04391123
ADAT3	0.58587345	0.717201381	0.816888346	0.047254211
ACTB	0.647072296	0.810281307	0.798577346	0.044339879
THOC1	0.462984356	0.693586112	0.668344294	0.011654486
POLR2I	0.606746348	0.74345152	0.816120933	0.041700246
DDX39B	0.698371702	1.029816486	0.678151604	0.002713309
EEF1A1	0.724377666	1.013037863	0.715054879	0.009425674
ENY2	0.616264306	1.233846378	0.499465993	0.006756721
PRMT5	0.410656167	0.506597053	0.810616969	0.022614807
METTL3	1.222689243	0.898248126	1.361193202	0.108763221
SMG7	1.269276228	0.971850534	1.306040574	0.27987272
DPH2	0.818452855	0.810958918	1.009240835	0.999400735
MED1	0.526051629	0.513278578	1.024885221	0.276012216
CELF1	0.542829121	0.677430913	0.801305507	0.104916932
BAZ1A	0.64786782	0.609606474	1.062764008	0.283275097
WDR43	0.533312303	0.528082318	1.00990373	0.181746661
DCAF1	0.488476224	0.515709978	0.947191726	0.073417582
RPS4X	0.405006532	0.474048313	0.854357079	0.221267126
POP1	0.66048718	0.584906758	1.129217898	0.524231104
LAGE3	0.693628646	0.701955509	0.988137621	0.175482784
TSEN34	0.717038063	0.699421915	1.025186726	0.175458122
RPS2	0.612578034	0.565698865	1.082869476	0.334795797
RPS18	0.573552917	0.557126179	1.029484771	0.235656703
PRPF19	0.605010456	0.522562535	1.157776182	0.682696046
MOCS3	0.847685787	0.65170713	1.30071584	0.42951301
EIF1	1.024728771	0.742409441	1.401193626	0.095204377
CAPRIN1	1.032563081	0.934271195	1.105207017	0.608980754
VIRMA	0.710379869	0.989120472	0.718243308	0.00116681
DHX9	0.985099461	0.706332758	1.394667669	0.000268141
DHX30	1.071454183	0.991026876	1.081155526	0.685925322
DHX36	0.986666408	1.412265051	0.698641099	0.008690912
HNRNPH3	1.186035857	1.039675034	1.140775548	0.609357953
CSNK1A1	0.8425	0.861743606	0.977668989	0.873765476
EIF3L	0.991956678	1.179310816	0.842678859	0.158438262
THOC5	0.747719406	0.662533365	1.128576228	0.448870284
THOC6	0.760219259	0.880153565	0.863734795	0.463818352
ABCE1	0.357540763	0.344434113	1.038052706	0.521060703

Table S2: Summary of siRNA validation in dual-luciferase reporters-GA frame. Related to Figure 1.

Gene name	C9R-Nluc fold change	AUG-Fluc fold change	Nluc/Fluc fold change	Nluc/Fluc p value
DDX3X	1.937518002	0.718388201	2.697034833	9.01782E-08
DPH5	2.645129812	1.49161514	1.773332638	0.000684715
DDX54	1.174711132	0.717251036	1.637796355	7.5562E-06
METTL14	1.530587434	0.930269585	1.645316001	0.000391177
DPH6	1.296373662	0.829425528	1.562977769	0.001379158
DHX29	1.367299686	0.854075037	1.606013998	0.001896146
DNAJC24	1.447331969	0.881605207	1.641700795	0.013040063
NXF1	0.239806403	1.040023531	0.230577862	1.4654E-06
NXT1	0.31914821	1.040134243	0.306833673	1.90243E-06
PSMA6	0.42922233	0.8225674	0.521808098	0.001052021
THOC3	0.699271915	1.15431843	0.605787708	0.004115584
THOC7	0.674500203	0.922329181	0.731300947	0.047817411
ADAT3	0.889843728	1.231004952	0.722859584	0.021425756
ACTB	0.789703241	1.040781177	0.758760111	0.016435843
THOC1	0.169829367	0.31661017	0.536398963	2.62009E-05
POLR2I	0.856072058	1.11621941	0.766938875	0.033971933
DDX39B	0.394100445	0.989140596	0.398427126	4.19576E-06
EEF1A1	0.45670178	0.801375786	0.569897155	2.58398E-05
ENY2	0.579192211	1.150615121	0.503376151	0.007025138
PRMT5	0.851686749	0.776719036	1.096518444	0.703458077
METTL3	2.748828513	1.879751381	1.462336212	0.003242797
SMG7	1.238731789	1.189489608	1.04139774	0.707590275
DPH2	1.149879211	1.372585341	0.83774697	0.118110248
MED1	0.776528629	0.805743097	0.963742205	0.524618618
CELF1	0.527147874	0.603056369	0.874127032	0.119865822
BAZ1A	0.805834931	0.985341946	0.817822619	0.016858423
WDR43	0.835926407	1.016519823	0.822341471	0.001687118
DCAF1	0.880242135	0.941659993	0.934777033	0.23525674
RPS4X	0.435542928	0.542391993	0.803003979	0.021633192
POP1	0.77634364	0.949524195	0.817613331	0.001898328
LAGE3	0.693628646	0.701955509	0.988137621	0.802115489
TSEN34	1.310586556	1.292490222	1.014001138	0.842854051
RPS2	1.068821552	0.95120801	1.1236465	0.53012949
RPS18	0.984609268	1.054689713	0.933553495	0.025396806
PRPF19	0.946084368	0.957580321	0.98799479	0.822484682
MOCS3	0.90872421	1.119922624	0.81141696	0.015506354
EIF1	1.044480755	1.330074541	0.785279864	0.069139446
CAPRIN1	0.790475735	0.863329919	0.915612581	0.241611197
VIRMA	2.286088802	1.826938397	1.251322325	0.041608657
DHX9	0.905245423	0.874358684	1.03279608	0.792016261
DHX30	0.857597854	1.007738411	0.85101237	0.268370478
DHX36	1.378670861	0.922329181	1.493532916	0.001793188
HNRNPH3	1.126317935	1.307281442	0.861572649	0.103725756
CSNK1A1	1.171267766	1.544052297	0.758567419	0.042864648
EIF3L	1.243373646	1.873307528	0.66373173	0.012209914
THOC5	1.107455575	0.955966694	1.155722792	0.16313791
THOC6				
ABCE1				

Table S3: Patient cell lines used in the study. Related to Methods.

Cell line ID	Line Name	ALS mutation	Gender
lymphoblast cell			
C9-ALS1	ND11411	C9ORF72 repeat expansion	Male
C9-ALS2	ND12455	C9ORF72 repeat expansion	Male
Control	38476	NA	NA
iPSCs			
C9-ALS1	CS7VCZiALS	C9ORF72 repeat expansion	Male
C9-ALS2	CS2YNLiALS	C9ORF72 repeat expansion	Male
C9-ALS3	CS0NKCiALS	C9ORF72 repeat expansion	Female
Control1	CS0594iCTR	NA	Female
Control2	CS8PAAiCTR	NA	Female
Control3	CS0702iCTR	NA	Male
iPSN			
C9-ALS1	CS2YNLiALS	C9ORF72 repeat expansion	Male
C9-ALS2	CS0NKCiALS	C9ORF72 repeat expansion	Female
C9-ALS3	CS0BUUiALS	C9ORF72 repeat expansion	Female
Control1	CS1ATZiCTR	NA	Male
Control2	CS8PAAiCTR	NA	Female
Control3	CS0702iCTR	NA	Male
Control4	CS0594iCTR	NA	Female

Table S4: qPCR primer sequences. Related to Methods.

Nluc	Forward	5'-GTCCGTAACTCCGATCCAAAG-3'
	Reverse	5'-TGCCATAGTGCAGGATCACCT-3'
Fluc	Forward	5'-GTGACTTCCCATTTGCCACC-3'
	Reverse	5'-TGATCTGGTTGCCGAAGATG-3'
Cluc	Forward	5'-TCTCTGGCCTCTGTGGAGAT-3'
	Reverse	5'-AACCGTCAAACTCCTGGTTG-3'
GAPDH mRNA	Forward	5'-GAGTCAACGGATTTGGTCGT-3'
	Reverse	5'-TTGATTTTGGAGGGATCTCG-3'
MT-RNR1	Forward	5'-CCCTGAAGCGCGTACACACC-3'
	Reverse	5'-GTCCAAGTGCACTTTCCAGT-3'
GAPDH pre-mRNA	Forward	5'-AAGGTGAAGGTCGGAGTCAAC-3'
	Reverse	5'-GCTGACCTTGAGCTCTCCTTG-3'
DDX3X	Forward	5'-TGCTGGCCTAGACCTGAACT-3'
	Reverse	5'-CCAAAACTGCTATACGCATCC-3'
C9ORF72 intron 1	Forward	5'-TCGCTGAGGGTGAACAAGAA-3'
	Reverse	5'-GCGCGCGACTCCTGAGT-3'
	Probe	5'-AAACAACCGCAGCCTGTAGCAAGCTC-3'